Biosensors and Bioelectronics 24 (2009) 3430–3435

Contents lists available at ScienceDirect

Biosensors and Bioelectronics

journal homepage: www.elsevier.com/locate/bios

Compact and low-cost biosensor based on novel approach to spectroscopy of surface plasmons☆

Marek Piliarik, Milan Vala, Ivo Tichý, Jiří Homola*

Institute of Photonics and Electronics ASCR, Chaberská 57, CZ-18251 Prague, Czech Republic

ARTICLE INFO

Article history:
Received 5 August 2008
Received in revised form 13 October 2008
Accepted 5 November 2008
Available online 17 November 2008

Keywords:
Surface plasmon resonance
Diffraction grating
Optical sensor
Biosensor

ABSTRACT

A high-performance surface plasmon resonance (SPR) sensor based on a novel approach to spectroscopy of surface plasmons is reported. This approach employs a special diffraction grating structure (referred to as surface plasmon resonance coupler and disperser, SPRCD) which simultaneously couples light into a surface plasmon and disperses the diffracted light for spectral readout of SPR signal. The developed SPRCD sensor consists of a miniature cartridge integrating the diffraction grating and microfluidics and a compact optical system which simultaneously acquires data from four independent sensing channels in the cartridge. It is demonstrated that the SPRCD sensor is able to measure bulk refractive index changes as small as 3×10^{-7} RIU (refractive index units) and to detect short oligonucleotides in concentrations down to 200 pM.

1. Introduction

Surface plasmon resonance (SPR) sensors represent one of the fastest developing label-free biosensor technologies with applications in biology, food safety, medical diagnostics, and environmental monitoring (Homola, 2008). However, high-resolution multichannel SPR sensors which are required for the most demanding biosensing applications are yet confined to laboratories primarily due to their large size, weight, power consumption, complexity and costs (Navratilova et al., 2007). In recent years several attempts have been made to develop portable SPR sensors (Soelberg et al., 2005; Chinowsky et al., 2007a; Kim et al., 2007; Chinowsky et al., 2007b; Feltis et al., 2008). The portable SPR sensors have been demonstrated for applications such as detection of pesticides in drinking water (Mauriz et al., 2006, 2007), detection of environmental toxic and endocrine disrupting compounds such as benzo[a]pyrene, 2,4-dichlorophenoxyacetic acid or atrazine (Dostálek et al., 2007; Farre et al., 2007; Kim et al., 2007) and detection of bacteria, spores and toxins (Chinowsky et al., 2007b). However, while high-performance laboratory SPR systems typically measure refractive index changes down to $(1–3) \times 10^{-7}$ (Homola, 2008), resolution of portable SPR sensors is typically significantly worse. With the exception of suitcase-size imaging SPR sensor reported by Chinowsky et al. (2007a) which delivers resolution of 5×10^{-7} RIU when averaging over large areas of a detector, compact SPR sensors provide refractive index resolution worse than 2×10^{-6} RIU (Chinowsky et al., 2007b; Kawazumi et al., 2005; Kim et al., 2007) which substantially limits their potential applications.

In this paper we present an SPR sensor based on a novel method of spectroscopy of surface plasmons which employs a special diffraction grating structure (referred to as surface plasmon resonance coupler and disperser, SPRCD) which simultaneously couples light into a surface plasmon and disperses the diffracted light for spectral readout. This approach allows construction of high-performance yet compact SPR sensors suitable for field use. A prototype of the sensor is presented and its detection capabilities are characterized in terms of refractive index resolution and ability to detect short oligonucleotides.

2. SPRCD sensor

2.1. Principle of operation

The principle of operation of the reported SPRCD sensor is based on recently demonstrated method of simultaneous excitation of surface plasmons and dispersion of diffracted light by means of a single diffraction grating – surface plasmon resonance coupler and disperser (Telezhnikova and Homola, 2006). In this approach polychromatic light wave illuminates a gold-coated diffraction grating under normal incidence through an adjacent dielectric medium (liquid sample). A portion of incident light is coupled to a surface plasmon at the metal–dielectric interface via the second order of diffraction. Simultaneously, the light diffracted into the first diffraction order is dispersed into wavelength components. The wavelength spectrum can then be obtained by investigating the

☆ This article is a part of the special issue "Biosensors 2008".

* Corresponding author. Tel.: +420 266 773 448; fax: +420 284 680 222.
E-mail address: homola@ufe.cz (J. Homola).

0956-5663/$ – see front matter © 2008 Elsevier B.V. All rights reserved.
doi:10.1016/j.bios.2008.11.003

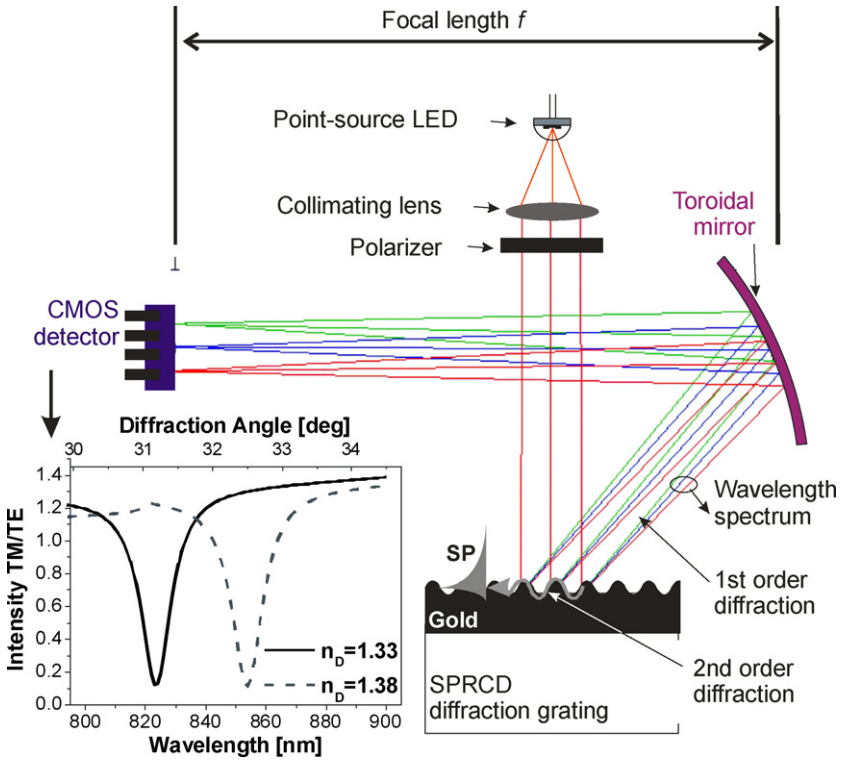

Fig. 1. Principle of SPRCD sensor.

angular spectrum of the diffracted light in the first order. The light energy transferred into a surface plasmon results in a drop in the intensity of light in the first diffraction order and can be observed as a sharp dip in the wavelength spectrum.

This concept has been implemented in a new sensing platform reported herein. In the geometry depicted in Fig. 1 an SPRCD diffraction grating is illuminated by a large-diameter collimated optical beam. The diffracted light is incident on the toroidal (or spherical) mirror which projects different angles of diffraction on different vertical positions in the back focal plane of the mirror where a detector records the spectrum of diffracted angles. The off-axis image on the detector depends on the perpendicular radius of the toroidal mirror.

2.2. Design and optimization

As follows from theoretical analysis (Homola and Piliarik, 2006), the ultimate performance of SPR sensors based on grating and prism couplers is comparable. Performance of the proposed SPRCD sensor depends on a variety of design parameters (*e.g.* grating profile, operating wavelength) and the performance of used components (*e.g.* light source and detector). We optimize design of the SPRCD sensor to achieve high sensor resolution and small dimensions of the optical bench, with respect to typical parameters of commercially available light sources and detectors. The minimum resolvable change in the refractive index (resolution of an SPR sensor) is determined by the following parameters: (i) the spectral width of the resonant dip, (ii) the depth of the resonant dip, (iii) the sensitivity of the resonant wavelength, (iv) the noise of the detector, and (v) the number of pixels of the detector. Noise properties of a detector depend on the detector design and used materials and fabrication technologies. These parameters have been carefully considered in the optimization analysis of the sensor presented in this study.

In this work, a rigorous integral method (Goray, 2005) was used to calculate spectra of diffracted light for different periods and modulation depths. In order to investigate the relationship between the design parameters and resolution of the SPRCD sensor, SPR spectra were combined with the model of detector shot-noise (Nenninger et al., 2002) and a figure of merit χ was calculated as

$$\chi = K\frac{S}{w}, \tag{1}$$

where S is sensitivity of the resonant wavelength to the unit change of refractive index, w the wavelength half-width of the SPR dip (Homola et al., 1999) and K is a geometrical parameter resulting from the distribution of the detector noise across the measured spectrum. As long as the shape of the dip on the detector does not change, the K-parameter remains constant. For each operating wavelength, the profile of the SPRCD grating was optimized in such a way that the figure of merit χ was maximized. The resulting wavelength dependences of the depth of modulation and period of the SPRCD grating are plotted in Fig. 2.

The minimum achievable dimension of the sensor system is limited by the focal length of the optics. The focal length is determined by the size of the detector and the interval of diffraction angles required to measure the changes of SPR spectrum. A 6.2 mm × 7.9 mm SXGA image detector was supposed in the system, as it is a typical size of CCD and CMOS cameras exhibiting desirable a noise/cost ratio. The angular spectrum of the diffracted light was modeled using PC Grate software and the focal length was calculated in such a way, that the half-width of the SPR dip covered 20% of the detector height (approximately 1 mm). Under these conditions, the operating range varies across the wavelength interval and becomes narrower at longer wavelengths. The operating range of at least 0.04 RIU can be achieved at wavelengths up to 950 nm.

Results of the instrumental optimization are summarized in Fig. 2. The figure of merit χ increases with the wavelength and within the considered wavelength range it increases by a factor of 5.5. This increase is associated with both increase of SPR sensitivity (approximately by 50%) and decrease of the spectral width of the SPR dip (almost threefold). Therefore, longer wavelengths are more suitable for the construction of high-performance SPRCD

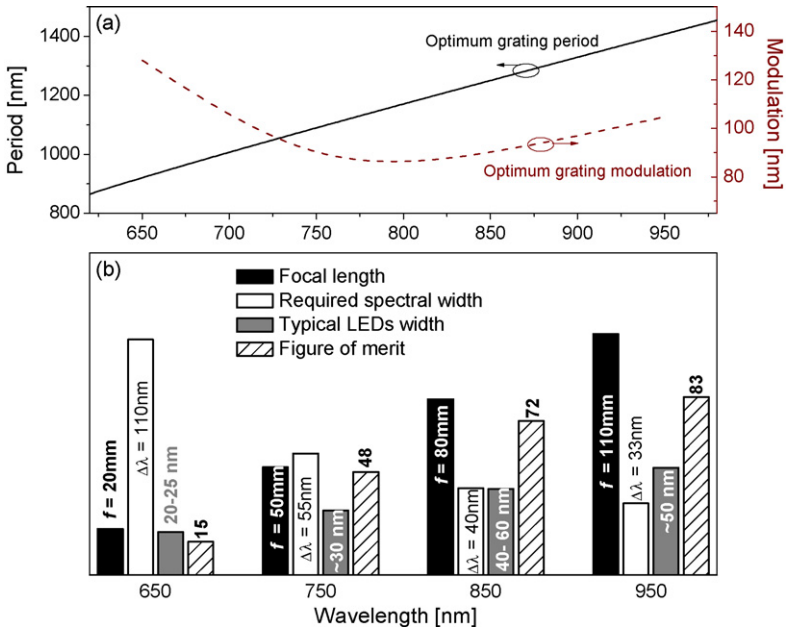

Fig. 2. (a) Wavelength dependence of the optimum SPRCD grating period and depth of modulation. (b) Focal length of the toroidal mirror, spectral width required for the SPRCD measurement, typical spectral width of an LED light source, and figure of merit, calculated for four different operating wavelengths.

sensor. The required focal length increases with the wavelength as a narrower range of diffracted angles needs to be involved at longer wavelengths. Therefore, a more compact SPRCD platform can be built when shorter wavelengths are utilized and above ~900 nm the focal length (the dimension of the optical bench cavity) exceeds 100 mm. On the other hand, the width of the wavelength spectrum decreases towards longer wavelength. Study of spectra of available light emitting diodes (LED) was performed (Hamamatsu Photonics, and Epitex, Inc., Japan) indicating that at wavelengths below 800 nm, emission spectra of available single chip LEDs are considerably narrower than required for the SPRCD operation. As follows from Fig. 2, the optimum operation of the SPRCD sensor is therefore achieved between 850 nm and 950 nm. As within this wavelength range the figure of merit χ changes only by 12% and the size of the optics (focal length) increases by 30%, we selected the wavelength of 850 nm for the construction of a prototype of SPRCD sensor.

2.3. Implementation

2.3.1. SPRCD optics

The layout of the SPRCD sensor optics is depicted in Fig. 1. Light from a point-source light emitting diode (psLED) (CLE332W from Clairex, Inc., USA) with a central wavelength of 850 nm and a spectral width of 40 nm was collimated using a plastic aspheric lens (focal length – 12.7 mm, from Edmund Optics GmbH, Germany), linearly polarized by a dichroic polarizer (ColorPol 700 BC4, Codixx, DE) and made incident on an SPRCD cartridge at the angle close to the normal incidence. Sensor cartridge included the SPRCD chip (the diffraction grating) with a set of microfluidic channels parallel to the plane of diffraction and a cover window through which the sensor chip was illuminated. The first order diffracted by the SPRCD was imaged by a toroidal mirror with perpendicular radii $r_1 = 50$ mm and $r_2 = 150$ mm (Dioptra, Czech Republic) on a CMOS detector (KAC-9638 from Kodak, USA). Electronic circuitry supporting the CMOS detector was integrated into the sensor body and connected with a PC via USB 2.0. The focus of the mirror in the axis parallel to the plane of diffraction (mirror radius 150 mm) was on the CMOS chip to provide the separation of wavelength components. In the perpendicular axis, the larger curvature of the mirror (radius 50 mm) provided point-to-point projection between the fluidic pattern cross-section and the CMOS detector. Prototype of the sensor optical bench was manufactured using 3D printer technology (Eden 250^{TM}, Objet Geometries Ltd.) from black epoxy (VeroBlack, Objet Geometries Ltd.). This method allowed development of a compact standalone sensor unit with the footprint smaller than 15 cm × 15 cm which incorporates optical bench, microfluidics and supporting electronics (Fig. 3). The wavelength calibration of the sensor was carried out using linear interpolation between the images of transmission windows of two laser line filters (central wavelengths of 850 nm and 830 nm, from Thorlabs Inc., USA).

2.3.2. Sensor cartridge

Holographic method was used to prepare SPRCD master grating (Dostálek et al., 2005) Prior to the holographic process, glass substrates (SF2 glass, from Schott, USA) were cleaned in acetone

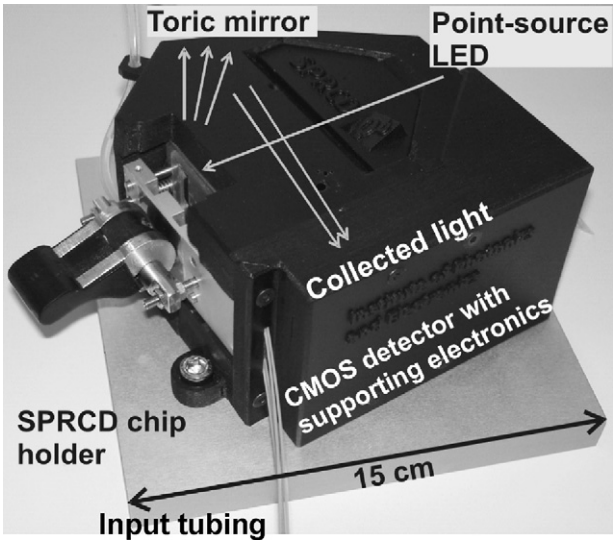

Fig. 3. Photograph of the SPRCD-based sensor with schematic drawing of light path inside the sensor.

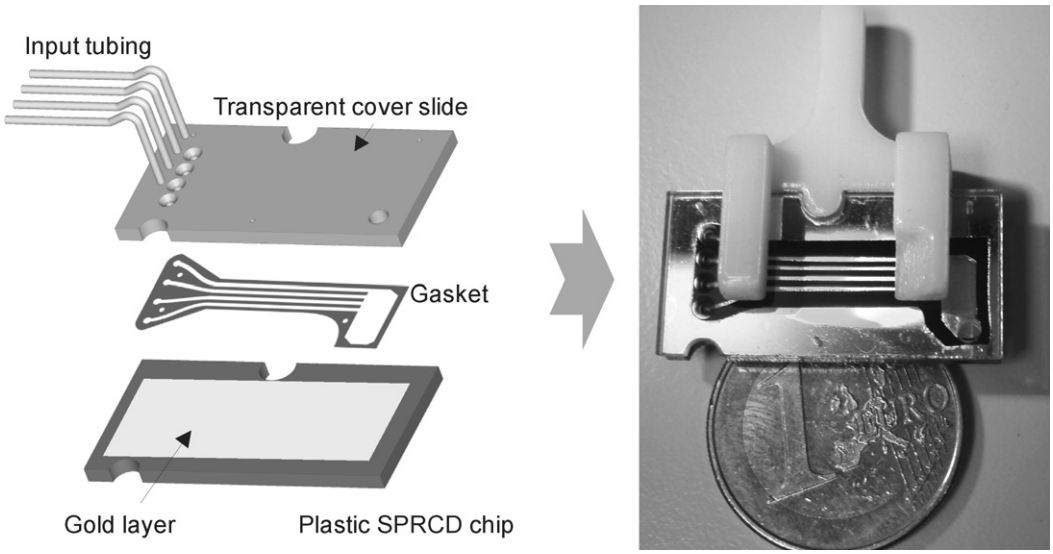

Fig. 4. SPRCD sensor cartridge. Scheme of main cartridge components and photograph of the assembled cartridge.

and in UV ozone cleaner (UVO model 42 from Jelight Company, USA) rinsed with ethanol and deionized (DI) water, and dried with stream of nitrogen. Substrates were spin-coated with positive photoresist (S1818 from Shipley, USA) and soft-baked for 15 min at 90 °C in hot-air oven resulting in about 2 μm thick photoresist layer. Coated substrates were exposed to two interfering collimated laser beams (He-Cd laser, λ = 442 nm, Liconix, USA) in Mach-Zehnder interferometer and then etched in AZ 303 developer (Microchemicals, Germany) to produce periodic corrugation. The surface relief of the master diffraction grating was transferred into optically flat polycarbonate substrates using hot-embossing technique (Optaglio, Czech Republic). Hot embossing is a conventional mass-production technology which allows rapid and low-cost production of large quantities of relief optical components in plastics (Gale, 1997) and is therefore is ideally suited for fabrication of low-cost SPRCD sensor chips. Rectangular SPRCD chips (dimensions: 15 mm × 30 mm) were cut from the polycarbonate substrate by means of a CO_2 laser. Finally, the chips were coated with a 100 nm thin gold film by the thermal evaporation in vacuum. The adhesion of gold to polycarbonate was promoted by a 5 nm thin titanium layer. Grating replicas were characterized by means of atomic force microscope (AFM, Multimode from Veeco, USA). The replicated gratings exhibited a modulation depth of 115 ± 10 nm and a period of 1249 nm.

The SPRCD chip was pressed against a transparent cover slide with gasket made of 100 μm thick self-adhesive plastic foil forming the SPRCD cartridge. Four 500 μm wide flow channels defined by the gasket were formed on the sensor surface in such a way that the direction of flow was perpendicular to the direction of grooves of the grating. Input and output ports were machined into the cover slide to interface with the sample delivery tubing in the sensor. The cartridge was kept together using a special clip to form an enclosed standalone and disposable unit. Components of the SPRCD sensor cartridge together with a photograph of the resulting cartridge are shown in Fig. 4. Peristaltic pump was used to flow liquid samples through the sensor cartridge.

2.3.3. Data processing

Images from a cropped area of the CMOS detector (480 × 980 pixels) were acquired at a frame-rate of 50 fps in 12-bit resolution. Then, the images were averaged over 100 frames by onboard electronics and resulting images were transmitted to a computer via USB link. Intensity spectra corresponding to the four sensing channels were observed as four bright bands in the image. Detector lines corresponding to each sensing channel were automatically recognized in the image by a software routine and the spectrum for each sensing channel was calculated as the average of these lines (the number of averaged lines per spectrum varied between 90 and 120). Reference spectra were recorded from the raw spectra while the SPRCD element was in contact with air. Normalized spectra were then calculated by dividing the raw spectra with the reference to compensate for unequal spectral distribution of light in the system. The position of the SPR dip was calculated by the least square fitting of a polynomial (2nd order) to a portion of the normalized spectrum below a fixed threshold.

3. Materials and methods

3.1. Reagents

The 16-mercapto-hexadecaoic acid ($HSC_{15}COOH$) and streptavidin from Streptomycea Avidinii were purchased from Sigma–Aldrich, USA. The 11-mercapto-(diethylenglycol)undecanol $HSC_{11}(EG)_2OH$ was purchased from Prochimia, Poland. The N,N,N′,N′-tetramethyl-O-(N-succinimidyl)uronium tetrafluoroborate (TSTU) (pure, ≥98%) was purchased from Sigma–Aldrich, USA. Absolute ethanol was purchased from MERCK, Czech Republic. The anhydrous N,N-dimethylformamide (DMF) (≥99.8%) was from Sigma–Aldrich, USA. The model deoxyribooligonucleotide probes used in this work biotin-(TEG)2-5′-d(CAG TGT GGA AAA TCT CTA GCA GT)-3′ (=BdO_{23}), and its complementary target 5′-d(ACT GCT AGA GAT TTT CCA CAC TG)-3′ (=CdO_{23}), were purchased from the Laboratory of Plant Molecular Physiology at Masaryk University in Brno, Czech Republic. The composition of buffer solutions used for streptavidin or oligonucleotide binding were as follows: PBS (1.4 mM KH_2PO_4, 8 mM $Na_2HPO_4{\cdot}12H_2O$, 137 mM NaCl, 2.7 mM KCl, pH 7.4 at 20 °C), PBM (1.4 mM KH_2PO_4, 8 mM $Na_2HPO_4{\cdot}12H_2O$, 15 mM $MgCl_2$, pH 7.4 at 20 °C), PBNa (1.4 mM KH_2PO_4, 8 mM $Na_2HPO_4{\cdot}12H_2O$, 0.75 M NaCl, 2.7 mM KCl, pH 7.4 at 20 °C), and SA (1 mM sodium acetate, pH 5.0 at 20 °C).

3.2. Sensor chip functionalization

Gold-coated sensor chip was cleaned using UV cleaner (Model 42, Jelight Company, USA), rinsed with ethanol and water and dried with nitrogen stream. Cleaned chips were immersed in a 3:1 mixture of $C_{11}(EG)_2$ and $C_{16}COOH$ alkanethiols dissolved in absolute

ethanol with a total thiol concentration of 1 mM for more than 12 h (alternatively, 4:1 mixture of absolute ethanol and DI water can be used as solvent). The carboxylic terminal groups on the sensor surface were activated for 2 h in N,N,N′,N′-tetramethyl-O-(N-succinimidyl)uronium tetrafluoroborate dissolved in dimethylformamide with a concentration of 2 mg/ml. Chips were rinsed with ethanol and deionized water, dried with nitrogen, assembled into the sensor cartridge and loaded into the SPRCD sensor. SA buffer solution with 50 μg/ml of streptavidin was flowed across the sensor surface for 15 min. Then, phosphate buffer was shortly flowed through the cartridge to remove non-covalently bound streptavidin and deactivate residual carboxylic groups. Finally, 50 nM solution of biotinylated oligonucleotides (BdO_{23}) in PBM buffer was flowed across the sensor surface for 15 min to allow attachment of biotinylated oligonucleotides to streptavidin via streptavidin–biotin interaction (Vaisocherová et al., 2006).

3.3. Refractometry

In order to quantify the sensor sensitivity to changes of bulk refractive index and to determine the sensor resolution, solutions of different concentrations of NaCl (0–10% solution in deionized water) were prepared. Refractive indices of the used solutions were characterized with temperature-stabilized refractometer DSR-lambda (Schmidt-Haensch, Germany) and were found in the interval of 1.3274 (water) to 1.3430 (at the wavelength of 820 nm). The refractive index samples were pumped through the flow-cell at a flow rate of 30 μl/min while the sensor response was recorded. Each sample was flowed through the flow-cell until a stable baseline was achieved (typically 3 min) and then the next solution was introduced.

3.4. Detection of oligonucleotides

In order to assess biosensing potential of the developed SPRCD sensor, model experiment was performed in which hybridization of short oligonucleotides in solution with complementary oligonucleotides immobilized on the sensor surface was observed. In this experiment the SPRCD sensor cartridge functionalized with oligonucleotide probe BdO_{23} was used. First, PBM buffer was pumped through the four flow-channels until the stable baseline was established. Then, a solution containing complementary oligonucleotide CdO_{23} was introduced into the system for 12 min and finally the sensor surface was washed with the PBM buffer until equilibrium signal was achieved. This experiment was carried out for five different concentrations of CdO_{23} (0.0 nM, 0.2 nM, 5 nM, 20 nM and 100 nM) dissolved in PBM buffer. The sensor response was recorded in real time in all four sensing channels.

4. Results and discussions

4.1. Refractometry

The temporal sensor responses recorded from four parallel sensing channels are shown in Fig. 5. The change of the refractive index of sample in the flow-cell resulted in a rapid shift of the resonant wavelength (the sensor response). The channel-to-channel reproducibility of sensor responses to the same change in refractive index was better than 5% which determines the consistency of SPR measurements in different channels with respect to the magnitude of the detected refractive index change. Reproducibility of sensor response in each sensing channel was better than 2% as follows from comparison of sensor responses to equal refractive indices (Fig. 5). This parameter characterizes the absolute accuracy of sensor readout. Based on the refractive index calibration the sensor sensitivity was determined to be 620 nm/RIU. As follows from

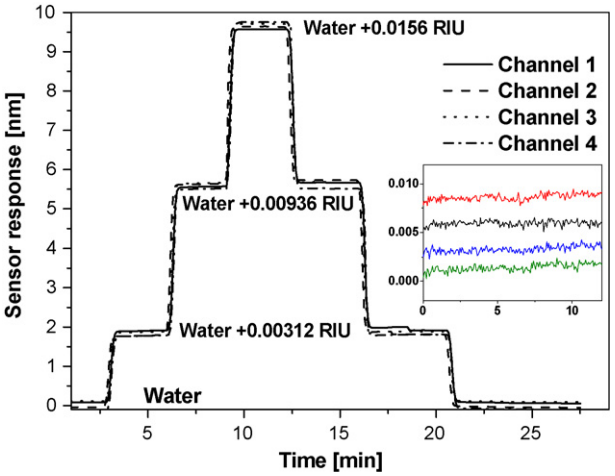

Fig. 5. SPRCD sensor response to four liquid samples with different refractive indices. Inset graph displays the baseline noise measured in four channels for 10 min (offset to zero).

theoretical analysis (Homola and Piliarik, 2006), sensitivity of grating-based SPR sensors varies by less than 0.5% within the used wavelength range (830–850 nm). The calibration curve determined for the SPRCD sensor follows this expected linear trend. The standard deviation of the baseline noise was 2×10^{-4} nm which corresponds to a refractive index resolution of 3×10^{-7} RIU.

The range of refractive indices covered by this calibration spans over 0.0156 RIU. The operating range of the sensor is determined by the spectral range imaged on the detector and the width of the SPR dip. The operating range of the demonstrated SPRCD sensor is approximately 0.02 RIU which is sufficient for the majority of biodetection applications. The operating range can be extended to almost 0.04 RIU with a changed crop setting on the image detector (this modification would decrease the detector frame rate and increase baseline noise). The demonstrated operating range (1.33–1.35 RIU) allows detection of binding events in aqueous solutions and common detection matrices (*e.g.* urine, blood plasma, blood serum, cerebrospinal fluid).

In order to investigate the crosstalk between two neighboring sensing channels a change in the refractive index was introduced into one channel. As there was no correlation between sensor responses from different channels (data not shown here), the inter-channel crosstalk was found negligible.

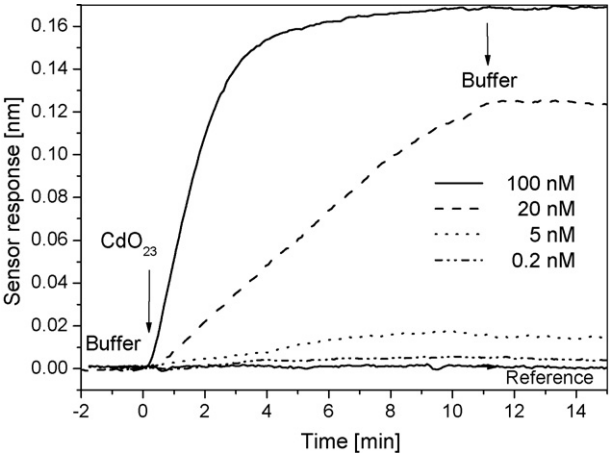

Fig. 6. Detection of oligonucleotides using an SPRCD sensor functionalized with oligonucleotide probes.

4.2. Detection of oligonucleotides

The kinetic responses of the SPRCD sensor to five different concentrations of CdO_{23} oligonucleotides are shown in Fig. 6. Solutions with target oligonucleotides complementary to immobilized probes induce a strong sensor response during a few minutes. The lowest resolvable concentration in this experiment was 200 pM. The detected sensor response corresponding to the 200 pM concentration was approximately 50 times lower than the saturation signal achieved for 100 nM concentration. As the affinity of the hybridization reaction is very high (affinity constant $> 10^8\ M^{-1}$), it can be assumed that the saturation signal observed for 100 nM oligonucleotide concentration corresponds to the hybridization of all of the immobilized probes. This result indicates that hybridization of as few as 2% of immobilized probes can be detected by the SPRCD sensor.

5. Conclusions

We demonstrated a new SPR biosensor based on novel approach to the spectroscopy of surface plasmons using a special diffraction grating. This approach allows simultaneous excitation of surface plasmons and dispersion of the diffracted light over a position-sensitive detector by a single diffraction grating (SPRCD). The SPRCD optics was designed and optimized in terms of performance and size of the optical bench. A laboratory prototype of the SPRCD sensor was built and evaluated in model refractometric experiments as well as in detection of biomolecular interactions taking place at the surface of the SPRCD chip. The achieved resolution of 3×10^{-7} RIU is comparable with the best laboratory commercial SPR sensors. The SPRCD biosensor was also demonstrated to be able to detect short oligonucleotides at concentrations as low as 200 pM.

Acknowledgement

This research was kindly supported by Phenogenomics Inc. (USA).

References

Chinowsky, T.M., Grow, M.S., Johnston, K.S., Nelson, K., Edwards, T., Fu, E., Yager, P., 2007a. Biosensors & Bioelectronics 22 (9–10), 2208–2215.
Chinowsky, T.M., Soelberg, S.D., Baker, P., Swanson, N.R., Kauffman, P., Mactutis, A., Grow, M.S., Atmar, R., Yee, S.S., Furlong, C.E., 2007b. Biosensors & Bioelectronics 22 (9–10), 2268–2275.
Dostálek, J., Homola, J., Miler, M., 2005. Sensors and Actuators B: Chemical 107 (1), 154–161.
Dostálek, J., Přibyl, J., Homola, J., Skládal, P., 2007. Analytical and Bioanalytical Chemistry 389 (6), 1841–1847.
Farre, M., Martinez, E., Ramon, J., Navarro, A., Radjenovic, J., Mauriz, E., Lechuga, L., Marco, M.P., Barcelo, D., 2007. Analytical and Bioanalytical Chemistry 388 (1), 207–214.
Feltis, B.N., Sexton, B.A., Glenn, F.L., Best, M.J., Wilkins, M., Davis, T.J., 2008. Biosensors & Bioelectronics 23 (7), 1131–1136.
Gale, M.T., 1997. Microelectronic Engineering 34 (3–4), 321–339.
Goray, L.I., 2005. Nuclear Instruments & Methods in Physics Research Section (a): Accelerators Spectrometers Detectors and Associated Equipment 536 (1–2), 211–221.
Homola, J., 2008. Chemical Reviews 108 (2), 462–493.
Homola, J., Koudela, I., Yee, S.S., 1999. Sensors and Actuators B: Chemical 54 (1–2), 16–24.
Homola, J., Piliarik, M., 2006. In: Homola, J. (Ed.), Surface Plasmon Resonance Based Sensors. Springer-Verlag, Berlin/Heidelberg/New York.
Kawazumi, H., Gobi, K.V., Ogino, K., Maeda, H., Miura, N., 2005. Sensors and Actuators B: Chemical 108 (1–2), 791–796.
Kim, S.J., Gobi, K.V., Iwasaka, H., Tanaka, H., Miura, N., 2007. Biosensors & Bioelectronics 23 (5), 701–707.
Mauriz, E., Calle, A., Manclus, J.J., Montoya, A., Hildebrandt, A., Barcelo, D., Lechuga, L.M., 2007. Biosensors & Bioelectronics 22 (7), 1410–1418.
Mauriz, E., Calle, A., Montoya, A., Lechuga, L.M., 2006. Talanta 69 (2), 359–364.
Navratilova, I., Papalia, G.A., Rich, R.L., Bedinger, D., Brophy, S., Condon, B., Deng, T., Emerick, A.W., Guan, H.W., Hayden, T., Heutmekers, T., Hoorelbeke, B., McCroskey, M.C., Murphy, M.M., Nakagawa, T., Parmeggiani, F., Qin, X.C., Rebe, S., Tomasevic, N., Tsang, T., Waddell, M.B., Zhang, F.F., Leavitt, S., Myszka, D.G., 2007. Analytical Biochemistry 364 (1), 67–77.
Nenninger, G.G., Piliarik, M., Homola, J., 2002. Measurement Science & Technology 13 (12), 2038–2046.
Soelberg, S.D., Chinowsky, T., Geiss, G., Spinelli, C.B., Stevens, R., Near, S., Kauffman, P., Yee, S., Furlong, C.E., 2005. Journal of Industrial Microbiology & Biotechnology 32 (11–12), 669–674.
Telezhnikova, O., Homola, J., 2006. Optics Letters 31 (22), 3339–3341.
Vaisocherová, H., Zítová, A., Lachmanová, M., Štěpánek, J., Králíková, S., Liboska, R., Rejman, D., Rosenberg, I., Homola, J., 2006. Biopolymers 82 (4), 394–398.